Glutamine Regulates the Human Epithelial Intestinal HCT-8 Cell Proteome under Apoptotic Conditions

Nicolas Deniel, Rachel Marion-Letellier, Roland Charlionet, François Tron, Jérôme Leprince, Hubert Vaudry, Philippe Ducrotté, Pierre Déchelotte, Sandrine Thébault

Glutamine Regulates the Human Epithelial Intestinal HCT-8 Cell Proteome under Apoptotic Conditions*[S]

Nicolas Deniel‡§, Rachel Marion-Letellier‡, Roland Charlionet¶, François Tron¶, Jérôme Leprince‖, Hubert Vaudry‖, Philippe Ducrotté‡, Pierre Déchelotte‡, and Sandrine Thébault‡§

Glutamine plays a key role in the metabolism of rapidly dividing cells, including enterocytes and lymphocytes, which may contribute to its beneficial clinical effects. Gut mucosal homeostasis is achieved through a balance between cell proliferation and apoptosis. In T cells, glutamine up-regulates antiapoptotic proteins and down-regulates proapoptotic proteins. In gut mucosa, glutamine prevents apoptosis in rat epithelial cell lines, whereas glutamine starvation induces apoptosis through caspase activation. Finally glutamine specifically prevents tumor necrosis factor-α-related apoptosis in the human intestinal cell line HT-29. Comparative functional proteomics enables the characterization of each differentially expressed protein in intestinal cells in response to modifications of nutritional environment. The influence of glutamine on intestinal proteome expression in apoptotic conditions has not been studied and evaluated. This comparative proteomics study was performed in the human epithelial intestinal cell line HCT-8 under experimental apoptotic conditions to investigate the influence of glutamine on protein expression during apoptosis. The pharmaconutritional effects of glutamine were determined under 2 mM (physiological concentration) and 10 mM (pharmaconutritional concentration) conditions. About 1,800 protein spots were revealed in both conditions. Comparative assessments indicated that 28 proteins were differentially expressed significantly (*i.e.* at least 2-fold modulated and Student's t test with $p \leq 0.05$) in response to an increase of glutamine concentration in the culture medium. Twenty-four proteins were identified by mass spectrometry and associated databases. From these proteins, 34% are involved in cell cycle and apoptosis mechanisms, 17% are involved in signal transduction, and 13% are involved in cytoskeleton organization. These data were integrated in a proposed schema of the interactome under apoptotic conditions. In conclusion, this study provides the first holistic picture of proteome modulation by glutamine in a human enterocytic cell line under apoptotic conditions and supports further evaluation of nutritional modulation of human intestinal proteome in various pathological conditions where apoptosis may be involved. *Molecular & Cellular Proteomics 6:1671–1679, 2007.*

Glutamine (Gln) is the most abundant free amino acid in the body and is essential for cell growth (1). As a non-essential amino acid, Gln is produced in sufficient quantities by most organs in physiological conditions but becomes a limiting, conditionally essential amino acid in severe catabolic states, such as major surgery, trauma, or sepsis (2). In such cases, endogenous Gln stores and synthesis decrease rapidly, resulting in Gln depletion, which is correlated with a poor prognosis (3). Recent studies have demonstrated the efficacy of Gln parenteral or enteral supplementation in reducing complication rates in critically ill and postoperative patients (4). Gln decreases bacteremia and enhances gut barrier function by stimulating enterocyte proliferation and intestinal protein synthesis (5). Gln is an energy substrate for most cells and conducts mitochondrial adenosine triphosphate formation. Gln also constitutes a precursor for nucleotides, glutamate, and especially glutathione synthesis (6). Gln is thus considered as the main respiratory fuel and metabolic precursor for rapidly dividing cells such as enterocytes and immune cells (6).

Gut mucosal homeostasis is achieved through a balance between cell proliferation, located in the crypt of Lieberkühn, and cell elimination by apoptosis, predominantly localized in both the crypt and villus compartment (7). In case of inflammatory bowel disease, the balance between proliferation and apoptosis is deregulated in inflamed or ulcerated area of gut mucosa (8).

At the molecular level, apoptosis is mainly orchestrated by the activation of the intracellular cysteine aspartate protease (caspase) cascade (9). Caspases are ubiquitously present in cells as latent precursors and constitute the molecular machinery for apoptosis (10). Two main apoptotic pathways leading to the activation of caspases have been described: the intrinsic pathway involving cytochrome *c* released from

mitochondria and the extrinsic pathway induced by several antibodies or ligands interacting with surface-exposed death receptors such as TNF[1] receptor-1. The first pathway is dependent on the process of mitochondrial outer membrane permeabilization regulated by pro- and antiapoptotic members of the Bcl-2 family (11). Concerning the extrinsic pathway, death receptor ligation leads to the formation of the death-inducing signaling complex and subsequently activation of procaspase-8 by autocatalysis (9). Both apoptosis pathways are connected notably via the proapoptotic Bid protein. *In fine*, caspase activation, especially caspase-3 activation, induces specific morphological and biochemical changes associated with the apoptotic cellular phenotype.

Gln could modulate apoptosis-related cellular mechanisms (12, 13). Indeed Gln up-regulates Bcl-2 and CD45RO antiapoptotic protein expression in lymphocytes and down-regulates the expression of Fas and Fas ligand proapoptotic proteins in the human T lymphocyte cell line Jurkat (14). In addition, Gln decreases both caspase-3 and caspase-8 activities in activated T cells (14).

The basic mechanisms of apoptotic signal transduction consist in quantitative and qualitative modifications of protein expression (10). Proteomics study of apoptotic cells allows us to determine the major biochemical actors and biomarkers of apoptosis under various environmental and pharmaconutritional conditions (15) including Gln supplementation (10). Consequently this study was designed to provide a holistic picture of protein modulations in Gln-treated (Gln concentration at 2 and 10 mM) human intestinal epithelial HCT-8 cells under CH11-induced apoptotic conditions.

EXPERIMENTAL PROCEDURES

Cell Cultures—Triplicate cultures of the human intestinal epithelial adenocarcinoma cell line HCT-8 (number 90032006, European Collection of Animal Cell Cultures, Salisbury, UK) were used between passages 44 and 46. Cell culture reagents, Dulbecco's modified Eagle's medium, Gln, non-essential amino acids, and fetal calf serum were supplied by Eurobio (Les Ulis, France). Tissue culture plates were obtained from ATGC (Noisy Le Grand, France). Cells were routinely grown as described previously (16). Culture medium without serum was used for stimulation for 24 h. Apoptosis was mediated with the mouse agonistic anti-Fas IgM monoclonal antibody CH11 used according to the manufacturer's instructions (Immunotech, Marseille, France). Cells were treated for 24 h with 125 ng/ml CH11 in 2 mM Gln (control) or in 10 mM Gln (Gln-treated), covering the range of physiological and pharmacological concentrations in these cells (16). Cells were washed three times with ice-cold PBS and isolated by scraping and centrifugation (360 × g for 5 min) at room temperature.

Protein Sample Preparation and Proteomics Assays—All reagents and instruments used have been described in detail previously (16).

---

[1] The abbreviations used are: TNF, tumor necrosis factor; 2-D, two-dimensional; IκB, inhibitor of nuclear factor κB; LMP, lysosomal membrane permeabilization; NF-κB, nuclear factor κB; PCD, programmed cell death; TGF-β, transforming growth factor-β; COMMD, copper metabolism gene MURR1 domain; ICAT, β-catenin-interacting protein 1; IKK, IκB kinase; MAP3K7, mitogen-activated protein kinase kinase kinase 7.

Protein quantification was performed with the 2-D Quant kit (Amersham Biosciences). Total protein lysates (450 μg) were loaded and resolved using commercial 18-cm IPG (3.5–10) strips (Amersham Biosciences) for the first dimension. The second dimension was performed on vertical polyacrylamide (Sigma-Aldrich) 8–16% (w/v) gradient slab gels (18 cm × 16 cm × 1.5 mm) and was run with a Laemmli SDS discontinuous system. Proteins were detected after Coomassie Brilliant Blue G-250 (Sigma-Aldrich) staining. The gels were destained for 2 h in 10% (v/v) methanol (Sigma-Aldrich) and 1% (v/v) acetic acid (Sigma-Aldrich) solutions. Gels were run in triplicates. The replicated gels were scanned (600 dots/inch resolution, 16 bits), and images were obtained with a computing and calibrating imaging densitometer (Model GS-700, Bio-Rad) and digitalization software (Multi-Analyst PC Software for the Bio-Rad Image Analysis Systems version 1.1, Bio-Rad).

Image Analysis—Differential analysis was performed using the ImageMaster[TM] 2D Platinum software version 5.0 (Amersham Biosciences) for spot detection, quantification, matching, and comparative analysis on a set of three simultaneously run gels per sample. The expression level was determined by the relative volume of each spot in the gel and expressed as %Volume (%Vol = (spot volume/∑volumes of all spots resolved in the gel)). This normalized spot volume takes into account variations due to protein loading and staining by considering the total volume over all the spots present in the gel. For each condition, two classes of gels were defined, namely class A for control samples (2 mM Gln) and class B for treated samples (10 mM Gln). Only groups of spots present in all gels were considered for differential analysis.

Statistical Analysis—To test the influence of 10 *versus* 2 mM Gln conditions, groupwise statistical comparisons were performed on groups of spots determined from triplicate gels both in 2 and 10 mM. Variations in abundance were calculated as the ratio of average values of %Vol for a group between the two classes. Only spots with a %Vol variation ratio greater than 2 (*i.e.* with significance set at ±2-fold change) in the ImageMaster 2D Platinum group report were considered relevant. The corresponding p values were determined using the Student's t test (significance level, $p \leq 0.05$) after spot %Vol log transformation. This process converts the distribution of %Vol from a non-normal distribution to a normal distribution. The corresponding prerequisites for this statistical test were carefully checked (17).

Automated In-gel Digestion of Protein, MALDI-TOF Mass Spectrometric Analysis, and Database Search Based on Peptide Mass Fingerprint Spectra—The 28 protein spots were automatically excised by cutting out from the gel using the Ettan[TM] Spot Picker (Amersham Biosciences) and digested on the Ettan Digester (Amersham Biosciences) with proteomics grade porcine trypsin (Sigma-Aldrich). After digestion the peptide mixtures were analyzed with a Voyager-DE[TM] MALDI-TOF mass spectrometer (Applied Biosystems, Foster City, CA) as described previously (16). All mass experiments were acquired in triplicate with α-cyano-4-hydroxycinnamic acid (LaserBio Labs, Sophia Antipolis, France) as matrix. The matrix peak relative to the CHCA $A_5K_3H^+$ form at 1060.0900 Da was excluded for peptide mass fingerprint analysis. External calibration was carried out using the peptide mixture "Proteomix-Peptide calibration Mix4" (LaserBio Labs). Moreover the tryptic autodigestion ion peaks (842.5100, 1045.5642, 2225.1202, and 2678.3822 Da) were used as internal standards to validate the external calibration procedure. This method typically resulted in mass accuracies of 80–120 ppm. For interpretation, each acquired spectrum was processed using Data Explorer version 4.0 (Applied Biosystems) with an advanced base-line correction (peak width, flexibility, and degree were fixed respectively at 32, 0.5, and 0.1) and noise removal (standard deviation to remove noise fixed at 2). A monoisotopic peptide mass list prepared from spectra
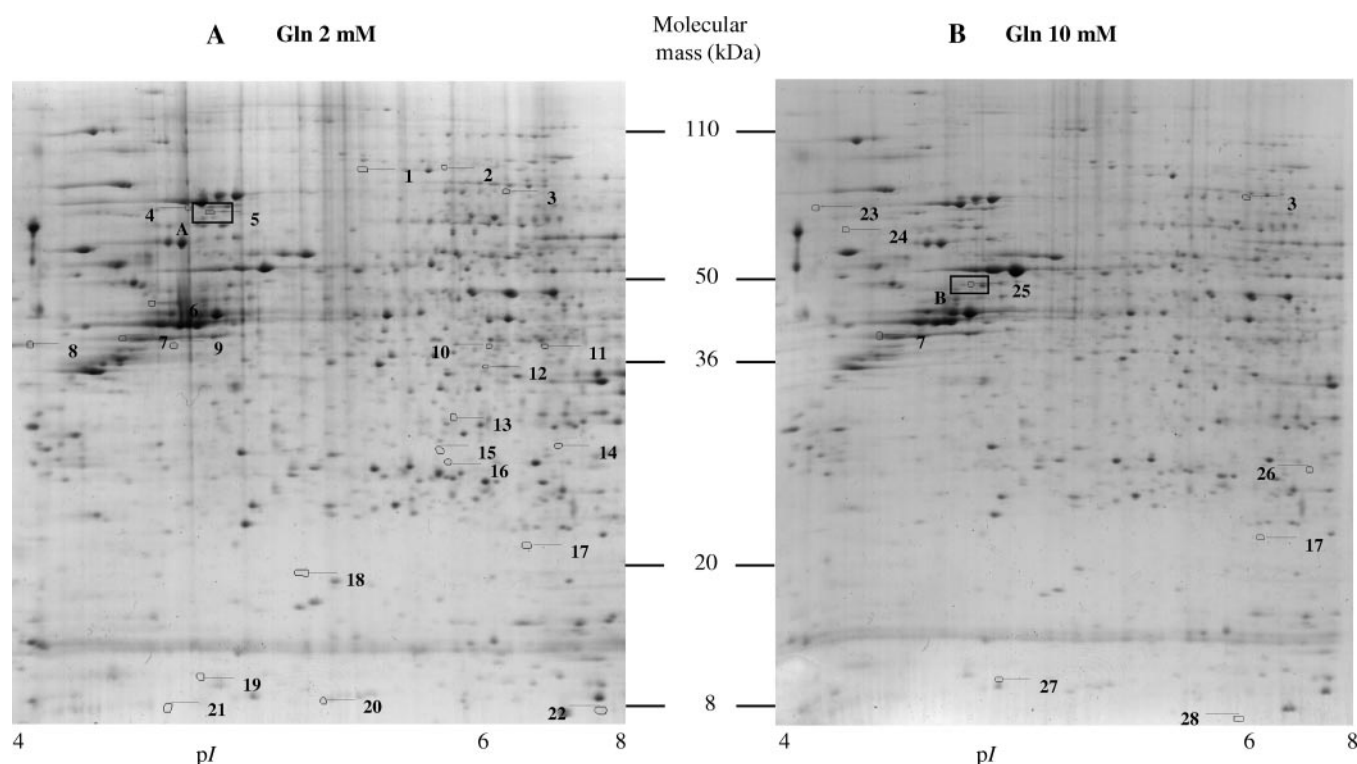
FIG. 1. **2-D gel images visualized by Coomassie Brilliant Blue staining representing total proteins extracted from HCT-8 under apoptotic conditions in 2 mM Gln (*A*) and 10 mM Gln (*B*).** The *numbered spots* were determined by statistical analysis and correspond to the proteins analyzed by MALDI-TOF MS and associated databases. Protein identification results are depicted in Table I.

was generated manually and put in the MS-Fit ProteinProspector search engine version 4.0.5 (developed in the University of California San Francisco Mass Spectrometry Facility). When using accurate masses from MALDI-TOF spectra as input data, Swiss-Prot release 50.0 of May 30, 2006 as database, a 100-ppm mass accuracy, trypsin as enzyme, allowance of one incomplete proteolytic cleavage site, cysteine carbamidomethylation, acrylamide-modified cysteine, methionine oxidation, selection of species (*Homo sapiens*), and similarity of pI and relative molecular mass were specified in the search program.

One-dimensional Western Blot Analysis—HCT-8 cell extracts were fractionated by 12% (w/v) SDS-PAGE, electroblotted onto nitrocellulose membranes, and incubated for 2 h with 1:5,000 (v/v) diluted rabbit anti-stathmin monoclonal antibody (Sigma-Aldrich) or with 1:1,000 (v/v) diluted goat anti-glucosidase II β subunit polyclonal antibody (Tebu, Le Perray en Yvelines, France). After washing, the membranes were probed with 1:10,000 (v/v) diluted peroxidase-conjugated rabbit or goat anti-IgG (Sigma-Aldrich) and revealed with an ECL system (Amersham Biosciences).

RESULTS

Gln-induced Effects on the Apoptotic HCT-8 Cell Proteome—Approximately 1,800 protein spots per gel were detected within a pI range of 3–10 and a relative molecular mass range of 10–150 kDa. 2-D gels obtained from cells exposed under apoptotic conditions in medium containing 2 or 10 mM Gln are presented in Fig. 1, *A* and *B*. Twenty-eight protein spots were differentially expressed. The proteins were identified with MALDI-TOF MS corresponding to 24 protein entries because four spots could not be identified with these spec-

trometric methods. Table I summarizes the identification results of these 28 proteins. Twenty protein spots from the apoptotic HCT-8 10 mM Gln class were decreased as compared with the control 2 mM Gln apoptotic HCT-8 cells. Eight protein spots were significantly up-regulated in 10 mM Gln-treated HCT-8 cells.

Biological Pathways Altered by 10 mM Gln Supplementation—Nineteen of the 20 down-regulated proteins, for example annexin 3 (spot 6), caspase-3 precursor (spot 12), glutathione *S*-transferase Mu 1 (spot 13), and stathmin (spot 18), were completely repressed when increasing the Gln concentration to 10 mM (Table I). Another protein exhibiting repressed expression, interleukin-1 receptor-associated kinase-like 2 (spot 5), is displayed in Fig. 2*A*. One of the four unidentified spots was down-regulated (Table I).

Among up-regulated proteins (Table I), six *de novo* expressions were observed, such as glucosidase II β subunit (spot 24), cell death regulator Aven (spot 7), and trans-Golgi network integral membrane protein 2 (spot 25) (Fig. 2*B*). 10 mM Gln also significantly up-regulated the expression level of the mitogen-activated protein kinase kinase 7 (spot 3).

Among the 28 spots influenced by Gln, 24 could be identified and classified. These proteins account for three major cellular functions. Pie charts (Fig. 3) representing the distribution of the Gln-altered proteins under apoptotic conditions indicate that 34% of the 10 mM Gln-regulated proteins (Fig. 3)

TABLE I

Comparison of HCT-8 cell line proteome under apoptotic conditions in response to 10 mM Gln treatment

Spot numbers with corresponding Swiss-Prot database accession number, the protein name, the main cellular function, the theoretical molecular mass and pI values, the spectrometric percentage of peptide/sequence coverage, and the modulation level are shown. App, appearance; Disp, disappearance; PRKX, protein kinase X.

Spot number	Accession number	Protein name	Function(s)	Theoretical pI	Theoretical molecular mass (kDa)	Expression level	Fold change	Peptide coverage / Sequence coverage (%)	Number of matched peaks	Number of unmatched peaks	Score on MS-Fit [a]
1	Q96LB3	Intraflagellar transport 74 homolog	Cytoskeleton	5.7	69.240	-	Disp	27/32	56	19	3.293×10^6
2	Q8WVM8	Sec1 family domain containing protein 1	Membrane trafficking	5.9	72.380	-	Disp	11/13	39	15	4.246×10^4
3	O43318	Mitogen-activated protein kinase kinase kinase 7	Signal transduction	6.7	67.797	+	2.102	19/4	41	16	8.457×10^3
4	Q96AY3	FK506-binding protein 10 [Precursor]	Protein biosynthesis and proteolysis	5.4	64.246	-	Disp	11/18	46	17	5.469×10^4
5	O43187	Interleukin-1 receptor-associated kinase-like 2	Signal transduction	5.7	55.271	-	Disp	7/14	28	14	7.668×10^4
6	P12429	Annexin A3	Cell cycle and apoptosis	5.6	36.244	-	Disp	11/11	49	17	3.845×10^4
7	Q9NQS1	Cell death regulator Aven	Cell cycle and apoptosis	4.9	38.506	+	3.430	14/14	42	15	6.302×10^4
8	P29966	Myristoylated alanine-rich C-kinase substrate	Cytoskeleton	4.5	31.545	-	Disp	11/25	25	12	2.155×10^5
9	Q9H1Y0	Autophagy protein 5	Cell cycle and apoptosis	5.5	32.448	-	Disp	6/17	23	12	1.006×10^5
10	P51817	Serine/threonine-protein kinase PRKX	Signal transduction	6.4	40.896	-	Disp	12/22	21	9	2.734×10^5
11	P50213	Isocitrate dehydrogenase [NAD] subunit α, mitochondrial [Precursor]	Carbohydrate metabolism	6.5	39.592	-	Disp	22/14	32	12	1.117×10^5
12	P42574	Caspase-3 [Precursor]	Cell cycle and apoptosis	6.1	31.594	-	Disp	26/18	24	13	7.428×10^5
13	P09488	Glutathione S-transferase Mu 1	Oxidative mechanisms	6.2	25.712	-	Disp	17/23	38	15	2.679×10^6
14	Q9BZ01	Putative FRG1-like protein c20orf80	Miscellaneous	7.0	20.762	-	Disp	26/29	27	11	6.229×10^6
15	P00492	Hypoxanthine–guanine phosphoribosyltransferase	Nucleic acid metabolism	6.2	24.580	-	Disp	22/27	28	10	4.150×10^6
16	Q86X83	COMM domain containing protein 2	Cell cycle and apoptosis	6.2	22.745	-	Disp	18/23	31	10	3.692×10^6
17	Undetermined	Undetermined	Undetermined	Undetermined	Undetermined	-	2.446	Undetermined	-	-	Undetermined
18	P16949	Stathmin	Cytoskeleton	5.8	17.303	-	Disp	26/40	88	20	5.004×10^7
19	O43715	TP53-regulated inhibitor of apoptosis 1	Cell cycle and apoptosis	5.4	8.786	-	Disp	18/34	74	18	2.627×10^6
20	Q9NSA3	Beta-catenin-interacting protein 1	Cell cycle and apoptosis	5.3	9.170	-	Disp	31/39	35	14	6.703×10^7
21	Q7Z4G1	COMM domain containing protein 6	Cell cycle and apoptosis	5.7	9.638	-	Disp	18/43	60	21	9.891×10^7
22	Q9UK08	Guanine nucleotide-binding protein G(I)/G(S)/G(O) γ-8 subunit	Signal transduction	6.6	7.841	-	Disp	17/17	68	19	1.544×10^5
23	Undetermined	Undetermined	Undetermined	Undetermined	Undetermined	+	App	Undetermined	-	-	Undetermined
24	P14314	Glucosidase II beta subunit [Precursor]	Protein biosynthesis and proteolysis	4.3	59.297	+	App	9/15	40	12	8.205×10^4
25	O43493	Trans-Golgi network integral membrane protein 2 [Precursor]	Membrane trafficking	5.5	51.007	+	App	14/16	51	14	6.600×10^4
26	Undetermined	Undetermined	Undetermined	Undetermined	Undetermined	+	App	Undetermined	-	-	Undetermined
27	P29762	Cellular retinoic acid binding protein 1	Lipid metabolism	5.3	15.566	+	App	11/14	27	11	9.746×10^4
28	Undetermined	Undetermined	Undetermined	Undetermined	Undetermined	+	App	Undetermined	-	-	Undetermined

[a] The score is defined as the Molecular Weight Search Score reported by MS-Fit and calculated as described through the MS-Fit ProteinProspector search engine developed in the University of California San Francisco Mass Spectrometry Facility.
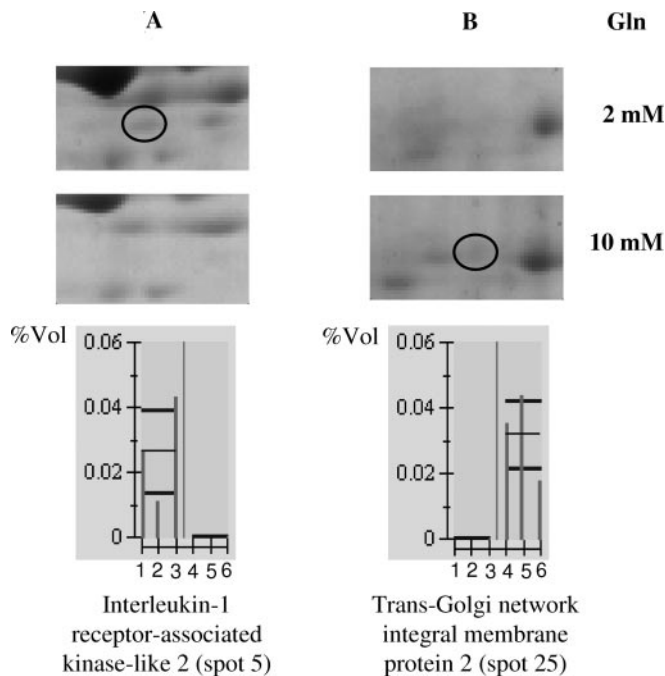
FIG. 2. **Enlargements of 2-D gels visualized by Coomassie Brilliant Blue staining.** In *A*, the *circle* represents the expression of spot 5 (interleukin-1 receptor-associated kinase-like 2) in 2 mM Gln (*top scan*) and its disappearance at 10 mM (*lower scan*). In *B*, the *circle* represents the *de novo* expression of spot 25 (trans-Golgi network integral membrane protein 2) between 2 mM (*top scan*) and 10 mM (*lower scan*). Integrated protein expressions as *histograms* are indicated for 2 mM Gln gels (*1*, *2*, and *3*) and 10 mM Gln gels (*4*, *5*, and *6*). The mean (*thin bar*) ± S.D. (*thick bar*) are indicated in *black*.
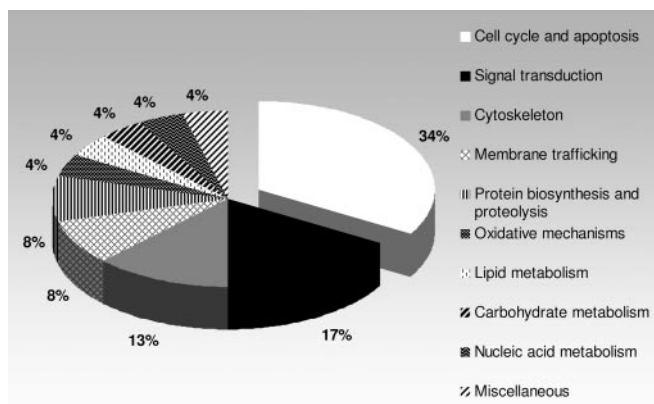

FIG. 3. **Pie charts representing the functional distribution of the differentially expressed HCT-8 proteins under apoptotic conditions after *in vitro* 10 mM Gln treatment.**

play a key role in cell cycle regulation, 17% play a key role in signal transduction, and 13% play a key role in cytoskeleton organization.

Specific Assessment of Two Gln-regulated Proteins by Western Blot Analysis—To further support protein identification according to the mass spectrum and substantiate their semiquantitative expression levels in 2 and 10 mM Gln conditions, antibodies against several of the Gln candidate targets
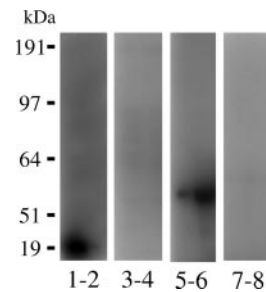

FIG. 4. **Immunoblot analysis of apoptotic HCT-8 cell extracts separated by SDS-PAGE.** Proteins were electroblotted onto nitrocellulose membranes and incubated with specific IgG (*lanes 1–4*, monoclonal IgG against stathmin; *lanes 5–8*, polyclonal IgG against glucosidase II β subunit). IgGs were revealed with their specific peroxidase-conjugated goat IgG. The immunoblots were developed using the ECL detection system. Negative controls were performed without incubating membranes with anti-stathmin or anti-glucosidase II β subunit antibodies. *Lane 1*, stathmin, 2 mM Gln; *lane 2*, stathmin, 10 mM Gln; *lane 3*, negative control, 2 mM Gln; *lane 4*, negative control, 10 mM Gln; *lane 5*, glucosidase II β subunit, 2 mM Gln; *lane 6*, glucosidase II β subunit, 10 mM Gln; *lane 7*, negative control, 2 mM Gln; *lane 8*, negative control, 10 mM Gln.

were used for Western blotting after separation of HCT-8 samples by SDS-PAGE. Fig. 4 shows that antibodies bound to stathmin (*lane 1*, stathmin, 2 mM Gln; *lane 2*, stathmin, 10 mM Gln) and glucosidase II β subunit (*lane 5*, glucosidase II β subunit, 2 mM Gln; *lane 6*, glucosidase II β subunit, 10 mM Gln). The corresponding negative controls are displayed in *lanes 3*, *4*, *7*, and *8*. These data confirmed the results given by 2-D gels and MS analysis.

Supplemental Data—Supplemental material is available in the on-line version of this article, including detailed spot %Vol measurements, statistical analysis, and mass spectrometry data relative to the 28 HCT-8 proteins significantly modified by Gln supplementation under apoptotic conditions.

DISCUSSION

The present study has demonstrated that high Gln concentration (10 mM), under apoptotic conditions, regulates the expression of several specific proteins mainly implicated in cell cycle, protein biosynthesis, and cytoskeleton organization processes, *i.e.* overall in cell life span and programmed cell death (PCD). A previous study has shown that Gln supplementation prevents spontaneous apoptosis in rat small intestine-derived epithelial cells, whereas Gln starvation induces apoptosis by caspase-3 and caspase-8 sequential activation (18). Moreover Gln prevented TNF-α-related apoptosis-inducing ligand effects in the human intestinal cell line HT-29 (19). The Gln-derived pyrimidine pathway appears to be tightly implicated in this process (20). Gln also prevents caspase-8 activation in human intestinal epithelial T84 cells cultured with the proapoptotic *Clostridium difficile* toxin A (21). Another potential mechanisms of Gln action is the pathway of glutathione, an antioxidant compound that detoxifies reactive oxygen species and has potent antiapoptotic effects (22, 23).

However, although the glutathione pathway is widely implicated in the antiapoptotic action of Gln on immune cells, Evans *et al.* (19) have demonstrated that this was not the case in the intestinal HT-29 cell line. Finally the protective effects of Gln on gut mucosa may be related to the induction of cytoprotective proteins, such as the heat shock protein (Hsp) family (24). For instance, Hsp-72 transcript and protein expression were up-regulated by Gln in IEC18 intestinal crypt-like epithelial cells during heat shock and apoptotic injury (25).

In our model, we induced apoptosis by using the mouse agonistic anti-Fas IgM monoclonal antibody CH11, which activates the Fas extrinsic pathway leading to death-inducing signaling complex constitution and to caspase-8 and caspase-10 activations. Extrinsic and intrinsic pathways are interconnected through considerable cross-talk leading to cell death (9). In particular, the Bid protein activates the mitochondrial pathway after cleavage by caspase-8 and finally amplifies the apoptotic process (9). The intrinsic pathway involves the formation of the heptameric apoptosome complex. In fact, once cytochrome *c* is released from mitochondria, it can bind the Apaf-1 protein and then recruit and activate procaspase-9 (11). The cell death regulator Aven, a novel antiapoptotic member, can bind both Bcl-xL and Apaf-1 (26). In the baby hamster kidney fibrosarcoma BHK cell line and in the human breast adenocarcinoma MCF-7 cell line, Aven interferes with the ability of Apaf-1 to self-associate and inhibits PCD induced by Apaf-1 and caspase-9 (26). Aven is broadly expressed and conserved in mammalian species (26). In addition, Aven enhances the protective antiapoptotic function of Bcl-xL in chinese hamster ovary cells (27). The present study demonstrated that 10 mM Gln up-regulates Aven expression and may therefore inhibit apoptosome formation and the end-step of mitochondrial-mediated apoptosis.

Extrinsic and intrinsic pathways, via caspase-8 and apoptosome, respectively, finally lead to the cleavage of procaspase-3. Once activated, caspase-3 orchestrates apoptosis through the cleavage of key substrates resulting in demolition and packaging of dying cells (28). Actually we observed in the present study that 10 mM Gln down-regulated the caspase-3 precursor expression in the HCT-8 cell line. In agreement with this finding, a previous study has shown that Gln inhibits activation of caspase-3 in Jurkat T cells stimulated with phorbol myristate acetate plus ionomycin (14). Moreover in the HT-29 human carcinoma cell line, Gln prevented the activation of caspase-3 in response to treatment with the TNF-α-related apoptosis-inducing ligand (19).

Mitogen-activated protein kinase kinase kinase 7 (MAP3K7), also called transforming growth factor-β (TGF-β)-activating kinase 1 (TAK1), is a key enzyme of the TGF-β pathway involved in the regulation of cell proliferation and differentiation in numerous cell types. Additionally MAP3K7 has been shown to modulate the Wnt/β-catenin signaling pathway via the nemo-like kinase activation in *Xenopus* embryos and human embryonic kidney HEK293 and DLD-1 human colon cancer cell lines. In these models, MAP3K7 stimulates nemo-like kinase activity and inhibits the interaction of the β-catenin and T cell factor-lymphoid enhancer factor nuclear factor transcriptional complex with deoxynucleotide nucleic acid (29–31). Actually aberrant accumulation of β-catenin protein due to mutations of either the β-catenin or adenomatous polyposis coli genes plays an essential role in the development of colorectal carcinoma (32). In the present work, Gln supplementation up-regulated MAP3K7 expression, and this effect may be involved in the modulation of HCT-8 extrinsic apoptosis by Gln. Moreover we observed that Gln down-regulated β-catenin-interacting protein 1 (ICAT) expression. ICAT negatively regulates Wnt signaling via β-catenin and T cell factor interaction inhibition (33). Because ICAT is overexpressed in almost half of colorectal carcinomas (33), nutritional modulation of ICAT could be an interesting approach to prevent the activation of inflammation leading to metaplasia and finally to cancer.

Furthermore we found that Gln down-regulated the expression of the COMMD (copper metabolism gene MURR1 domain) proteins 2 and 6. These proteins belong to the recently discovered COMMD protein family. COMMD proteins are extensively conserved in multicellular eukaryotic organisms and establish multimeric complexes involved in NF-κB transcriptional inhibition (34, 35). In physiological conditions, NF-κB is sequestered in the cytoplasm through an interaction with a family of inhibitory proteins, the inhibitor of nuclear factor κB (IκB). IκB proteins are phosphorylated by the IκB kinase (IKK) complex. After ubiquitinylation, IκB proteins are rapidly degraded by the proteasome, and this finally allows nuclear translocation and activation of NF-κB (36). NF-κB stimulates cell proliferation and limits PCD in different cell types, including rat IE6 cells (37, 38). Several studies have demonstrated that MAP3K7 activates IKK following TGF-β1 treatment in murine hepatocytes (39) or TNF-α treatment in HeLa cells (40). Thus, Gln appears to positively modulate the antiapoptotic effects of NF-κB both by inducing the MAP3K7/IKK pathway and by decreasing the expression of both COMMD 2 and 6 NF-κB inhibitors.

Stathmin, or oncoprotein 18, is a ubiquitous cytoplasmic protein implicated in the dynamic regulation of microtubules. Stathmin promotes microtubule depolymerization during interphase and late mitosis and is regulated by changes in phosphorylation levels during cell cycle progression (41). Accordingly stathmin phosphorylation inhibits the protein microtubule destabilizing activity (41). Stathmin expression is up-regulated in a wide variety of human cancers such as acute leukemia and breast and liver cancer (42). Recently stathmin has been found to be activated by the apoptosis signal-regulating kinase 1-p38 cascade in rat pheochromocytoma PC12 cells (43). Here we observed that stathmin expression was down-regulated in HCT-8 cells, suggesting that Gln supplementation potentially modulates microtubule stabilization under apoptotic conditions.
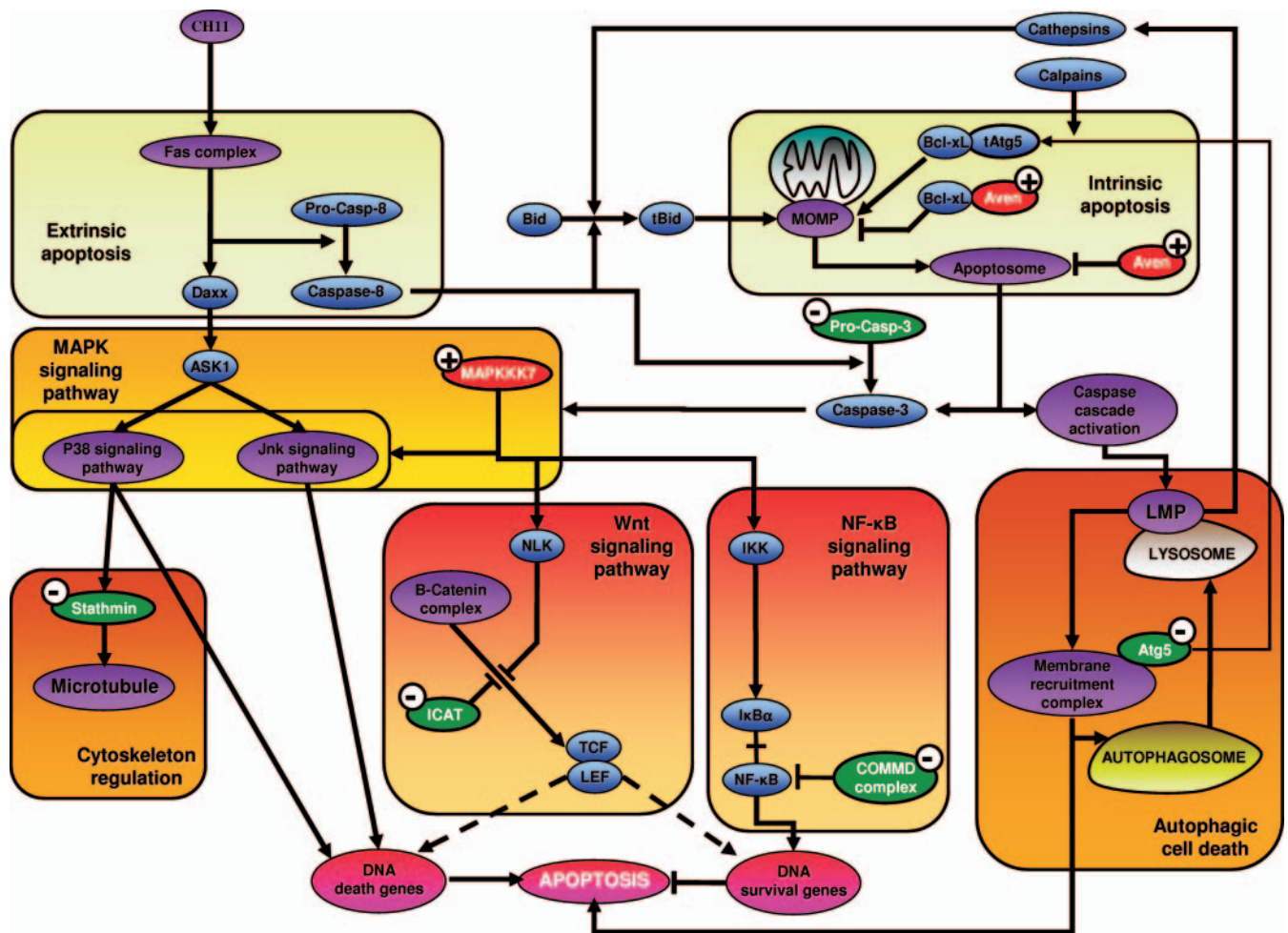
FIG. 5. **Schematic representation of seven relevant Gln-modulated protein interactions in the HCT-8 human epithelial cell line under CH11 experimental apoptotic conditions.** Up-regulated and down-regulated proteins are indicated with + (*red*) and − (*green*), respectively. The interactions are indicated with *lines*. *tAtg5* and *tBib* indicate truncated forms of the corresponding proteins. *ASK1*, apoptosis signal-regulating kinase 1; *MOMP*, mitochondrial outer membrane permeabilization; *NLK*, nemo-like kinase; *TCF*, T cell factor; *LEF*, lymphoid enhancer factor; *Casp*, caspase; *MAPK*, mitogen-activated protein kinase; *Jnk*, c-Jun NH$_2$-terminal kinase.

Autophagy consists in wrapping a part of the cytoplasm into a specific membrane and to its later digestion by lysosomal enzymes. Depending on the cellular context, autophagy can promote cell survival or induce cell death in response to endogenous and exogenous stress, such as apoptotic effectors. It is generally accepted that during these cell death conditions, lysosomal membrane permeabilization (LMP) induces cytotoxic effects and is related to activation of the mitochondrial cell death pathway (44). Actually the proapoptotic protein Bid can be cleaved by cathepsins or lysosomal proteases in HeLa cells and human breast cancer MCF-7 cells (45, 46). Consequently Bid seems to be implicated as a potential mediator connecting LMP and autophagy (PCD type II) to apoptosis (PCD type I) processes. In addition, after TNF-α induction, LMP requires the caspase-8-mediated pathway in mice hepatocytes (47). Interestingly in our model, the expression of a protein involved in autophagy, Atg5, was markedly down-regulated by 10 mM Gln, suggesting that Gln supple-

mentation can negatively modulate not only PCD type 1 (apoptosis) but also PCD type 2 (autophagy-mediated cell death). Autophagy is notably controlled by an evolutionarily conserved protein family, the autophagy proteins (Atg) (48). Sixteen Atg proteins are involved in the autophagosome biogenesis. Autophagosome represents the initial vacuole that sequesters cytoplasmic material before its delivery to the lysosome, and the (Atg12-Atg5-Atg16)$_4$ tetramer complex is required for autophagosome expansion and completion (48). Moreover previous studies demonstrated the involvement of the Atg5 protein in autophagic cell death (49, 50). Accordingly the interaction between Atg5 and FADD (Fas-associated protein with death domain) has been shown to play a crucial role in interferon-γ-induced cell death (51). A recent study has demonstrated that Atg5 constitutes a substrate for calpains 1 and 2 in several cell types (52). Actually the truncated form of Atg5 (relative molecular mass of 24,000 Da) tightly interacts with Bcl-xL, leading to antiapoptotic protein inactivation (49,

52). Thus, we demonstrate for the first time that Atg5 protein expression and consequently autophagic cell death mechanisms can be modulated by Gln supplementation. These data provide crucial information to understand the regulatory pathways of this recently discovered proapoptotic protein.

Altogether our results provide new interesting leads to explain the apoptosis suppressive capacities of Gln. The differentially expressed proteins described above are tightly implicated in all of the apoptotic processes including the extrinsic (MAP3K7 plus downstream effectors) and intrinsic apoptosis pathway (Aven), autophagy (Atg5), and cytoskeleton regulation (stathmin). Based on these results and a bibliographic analysis, the Gln-modulated protein data described above can be integrated to provide a global schema of the intestinal interactome under apoptotic conditions (Fig. 5) depicting the relevant protein interactions and the subcellular pathways involved that ultimately contribute to the cytoprotective effects of Gln. Finally our work introduces new ways of investigation for further research involving the antiapoptotic mechanisms of Gln in intestinal cells and may lead to the discovery of new biomarkers for the understanding of inflammation as well as cancer initiation and progression.

REFERENCES

1. Labow, B. I., and Souba, W. W. (2000) Glutamine. *World J. Surg.* **24,** 1503–1513
2. Melis, G. C., ter Wengel, N., Boelens, P. G., and van Leeuwen, P. A. (2004) Glutamine: recent developments in research on the clinical significance of glutamine. *Curr. Opin. Clin. Nutr. Metab. Care* **7,** 59–70
3. Coeffier, M., and Dechelotte, P. (2005) The role of glutamine in intensive care unit patients: mechanisms of action and clinical outcome. *Nutr. Rev.* **63,** 65–69
4. Reeds, P. J., and Burrin, D. G. (2001) Glutamine and the bowel. *J. Nutr.* **131,** (suppl.) 2505S–2508S, discussion 2523S–2504S
5. Coeffier, M., Claeyssens, S., Hecketsweiler, B., Lavoinne, A., Ducrotte, P., and Dechelotte, P. (2003) Enteral glutamine stimulates protein synthesis and decreases ubiquitin mRNA level in human gut mucosa. *Am. J. Physiol.* **285,** G266–G273
6. Curi, R., Lagranha, C. J., Doi, S. Q., Sellitti, D. F., Procopio, J., Pithon-Curi, T. C., Corless, M., and Newsholme, P. (2005) Molecular mechanisms of glutamine action. *J. Cell. Physiol.* **204,** 392–401
7. Bach, S. P., Renehan, A. G., and Potten, C. S. (2000) Stem cells: the intestinal stem cell as a paradigm. *Carcinogenesis* **21,** 469–476
8. Radtke, F., and Clevers, H. (2005) Self-renewal and cancer of the gut: two sides of a coin. *Science* **307,** 1904–1909
9. Zimmermann, K. C., Bonzon, C., and Green, D. R. (2001) The machinery of programmed cell death. *Pharmacol. Ther.* **92,** 57–70
10. Thiede, B., and Rudel, T. (2004) Proteome analysis of apoptotic cells. *Mass Spectrom. Rev.* **23,** 333–349
11. Green, D. R. (2005) Apoptotic pathways: ten minutes to dead. *Cell* **121,** 671–674
12. Fuchs, B. C., and Bode, B. P. (2006) Stressing out over survival: glutamine as an apoptotic modulator. *J. Surg. Res.* **131,** 26–40
13. Mates, J. M., Segura, J. A., Alonso, F. J., and Marquez, J. (2006) Pathways from glutamine to apoptosis. *Front. Biosci.* **11,** 3164–3180
14. Chang, W. K., Yang, K. D., Chuang, H., Jan, J. T., and Shaio, M. F. (2002) Glutamine protects activated human T cells from apoptosis by upregulating glutathione and Bcl-2 levels. *Clin. Immunol.* **104,** 151–160
15. Lenaerts, K., Renes, J., Bouwman, F. G., Noben, J. P., Robben, J., Smit, E., and Mariman, E. C. (2007) Arginine deficiency in preconfluent intestinal Caco-2 cells modulates expression of proteins involved in proliferation, apoptosis, and heat shock response. *Proteomics* **7,** 565–577
16. Thebault, S., Deniel, N., Marion, R., Charlionet, R., Tron, F., Cosquer, D., Leprince, J., Vaudry, H., Ducrotte, P., and Dechelotte, P. (2006) Proteomic analysis of glutamine-treated human intestinal epithelial HCT-8 cells under basal and inflammatory conditions. *Proteomics* **6,** 3926–3937
17. Chich, J. F., David, O., Villers, F., Schaeffer, B., Lutomski, D., and Huet, S. (2007) Statistics for proteomics: experimental design and 2-DE differential analysis. *J. Chromatogr. B Anal. Technol. Biomed. Life Sci.* **849,** 261–272
18. Papaconstantinou, H. T., Chung, D. H., Zhang, W., Ansari, N. H., Hellmich, M. R., Townsend, C. M., Jr., and Ko, T. C. (2000) Prevention of mucosal atrophy: role of glutamine and caspases in apoptosis in intestinal epithelial cells. *J. Gastrointest. Surg.* 4, 416–423
19. Evans, M. E., Jones, D. P., and Ziegler, T. R. (2003) Glutamine prevents cytokine-induced apoptosis in human colonic epithelial cells. *J. Nutr.* **133,** 3065–3071
20. Evans, M. E., Jones, D. P., and Ziegler, T. R. (2005) Glutamine inhibits cytokine-induced apoptosis in human colonic epithelial cells via the pyrimidine pathway. *Am. J. Physiol.* **289,** G388–G396
21. Carneiro, B. A., Fujii, J., Brito, G. A., Alcantara, C., Oria, R. B., Lima, A. A., Obrig, T., and Guerrant, R. L. (2006) Caspase and bid involvement in Clostridium difficile toxin A-induced apoptosis and modulation of toxin A effects by glutamine and alanyl-glutamine in vivo and in vitro. *Infect. Immun.* **74,** 81–87
22. Mates, J. M., Perez-Gomez, C., Nunez de Castro, I., Asenjo, M., and Marquez, J. (2002) Glutamine and its relationship with intracellular redox status, oxidative stress and cell proliferation/death. *Int. J. Biochem. Cell Biol.* **34,** 439–458
23. Roth, E., Oehler, R., Manhart, N., Exner, R., Wessner, B., Strasser, E., and Spittler, A. (2002) Regulative potential of glutamine—relation to glutathione metabolism. *Nutrition* **18,** 217–221
24. Wischmeyer, P. E. (2002) Glutamine and heat shock protein expression. *Nutrition* **18,** 225–228
25. Ropeleski, M. J., Riehm, J., Baer, K. A., Musch, M. W., and Chang, E. B. (2005) Anti-apoptotic effects of L-glutamine-mediated transcriptional modulation of the heat shock protein 72 during heat shock. *Gastroenterology* **129,** 170–184
26. Chau, B. N., Cheng, E. H., Kerr, D. A., and Hardwick, J. M. (2000) Aven, a novel inhibitor of caspase activation, binds Bcl-xL and Apaf-1. *Mol. Cell* **6,** 31–40
27. Figueroa, B., Jr., Chen, S., Oyler, G. A., Hardwick, J. M., and Betenbaugh, M. J. (2004) Aven and Bcl-xL enhance protection against apoptosis for mammalian cells exposed to various culture conditions. *Biotechnol. Bioeng.* **85,** 589–600
28. Wang, Z. B., Liu, Y. Q., and Cui, Y. F. (2005) Pathways to caspase activation. *Cell Biol. Int.* **29,** 489–496
29. Ishitani, T., Ninomiya-Tsuji, J., Nagai, S., Nishita, M., Meneghini, M., Barker, N., Waterman, M., Bowerman, B., Clevers, H., Shibuya, H., and Matsumoto, K. (1999) The TAK1-NLK-MAPK-related pathway antagonizes signalling between β-catenin and transcription factor TCF. *Nature* **399,** 798–802
30. Ishitani, T., Kishida, S., Hyodo-Miura, J., Ueno, N., Yasuda, J., Waterman, M., Shibuya, H., Moon, R. T., Ninomiya-Tsuji, J., and Matsumoto, K. (2003) The TAK1-NLK mitogen-activated protein kinase cascade functions in the Wnt-5a/Ca^{2+} pathway to antagonize Wnt/β-catenin signaling. *Mol. Cell. Biol.* **23,** 131–139
31. Yasuda, J., Tsuchiya, A., Yamada, T., Sakamoto, M., Sekiya, T., and Hirohashi, S. (2003) Nemo-like kinase induces apoptosis in DLD-1 hu-

man colon cancer cells. *Biochem. Biophys. Res. Commun.* **308,** 227–233

32. Giles, R. H., van Es, J. H., and Clevers, H. (2003) Caught up in a Wnt storm: Wnt signaling in cancer. *Biochim. Biophys. Acta* **1653,** 1–24

33. Koyama, T., Tago, K., Nakamura, T., Ohwada, S., Morishita, Y., Yokota, J., and Akiyama, T. (2002) Mutation and expression of the β-catenin-interacting protein ICAT in human colorectal tumors. *Jpn. J. Clin. Oncol.* **32,** 358–362

34. Burstein, E., Hoberg, J. E., Wilkinson, A. S., Rumble, J. M., Csomos, R. A., Komarck, C. M., Maine, G. N., Wilkinson, J. C., Mayo, M. W., and Duckett, C. S. (2005) COMMD proteins, a novel family of structural and functional homologs of MURR1. *J. Biol. Chem.* **280,** 22222–22232

35. de Bie, P., van de Sluis, B., Burstein, E., Duran, K. J., Berger, R., Duckett, C. S., Wijmenga, C., and Klomp, L. W. (2006) Characterization of COMMD protein-protein interactions in NF-κB signalling. *Biochem. J.* **398,** 63–71

36. Viatour, P., Merville, M. P., Bours, V., and Chariot, A. (2005) Phosphorylation of NF-κB and IκB proteins: implications in cancer and inflammation. *Trends Biochem. Sci.* **30,** 43–52

37. Potoka, D. A., Upperman, J. S., Nadler, E. P., Wong, C. T., Zhou, X., Zhang, X. R., and Ford, H. R. (2002) NF-κB inhibition enhances peroxynitrite-induced enterocyte apoptosis. *J. Surg. Res.* **106,** 7–14

38. Biswas, D. K., Martin, K. J., McAlister, C., Cruz, A. P., Graner, E., Dai, S. C., and Pardee, A. B. (2003) Apoptosis caused by chemotherapeutic inhibition of nuclear factor-κB activation. *Cancer Res.* **63,** 290–295

39. Arsura, M., Panta, G. R., Bilyeu, J. D., Cavin, L. G., Sovak, M. A., Oliver, A. A., Factor, V., Heuchel, R., Mercurio, F., Thorgeirsson, S. S., and Sonenshein, G. E. (2003) Transient activation of NF-κB through a TAK1/IKK kinase pathway by TGF-beta1 inhibits AP-1/SMAD signaling and apoptosis: implications in liver tumor formation. *Oncogene* **22,** 412–425

40. Takaesu, G., Surabhi, R. M., Park, K. J., Ninomiya-Tsuji, J., Matsumoto, K., and Gaynor, R. B. (2003) TAK1 is critical for IκB kinase-mediated activation of the NF-κB pathway. *J. Mol. Biol.* **326,** 105–115

41. Andersen, S. S. (2000) Spindle assembly and the art of regulating microtubule dynamics by MAPs and Stathmin/Op18. *Trends Cell Biol.* **10,** 261–267

42. Mistry, S. J., and Atweh, G. F. (2002) Role of stathmin in the regulation of the mitotic spindle: potential applications in cancer therapy. *Mt. Sinai J. Med.* **69,** 299–304

43. Mizumura, K., Takeda, K., Hashimoto, S., Horie, T., and Ichijo, H. (2006) Identification of Op18/stathmin as a potential target of ASK1-p38 MAP kinase cascade. *J. Cell. Physiol.* **206,** 363–370

44. Kroemer, G., and Jaattela, M. (2005) Lysosomes and autophagy in cell death control. *Nat. Rev. Cancer* **5,** 886–897

45. Cirman, T., Oresic, K., Mazovec, G. D., Turk, V., Reed, J. C., Myers, R. M., Salvesen, G. S., and Turk, B. (2004) Selective disruption of lysosomes in HeLa cells triggers apoptosis mediated by cleavage of Bid by multiple papain-like lysosomal cathepsins. *J. Biol. Chem.* **279,** 3578–3587

46. Lamparska-Przybysz, M., Gajkowska, B., and Motyl, T. (2005) Cathepsins and BID are involved in the molecular switch between apoptosis and autophagy in breast cancer MCF-7 cells exposed to camptothecin. *J. Physiol. Pharmacol.* **56,** Suppl, 3, 159–179

47. Werneburg, N., Guicciardi, M. E., Yin, X. M., and Gores, G. J. (2004) TNF-α-mediated lysosomal permeabilization is FAN and caspase 8/Bid dependent. *Am. J. Physiol.* **287,** G436–G443

48. Klionsky, D. J. (2005) The molecular machinery of autophagy: unanswered questions. *J. Cell Sci.* **118,** 7–18

49. Codogno, P., and Meijer, A. J. (2006) Atg5: more than an autophagy factor. *Nat. Cell Biol.* **8,** 1045–1047

50. Shimizu, S., Kanaseki, T., Mizushima, N., Mizuta, T., Arakawa-Kobayashi, S., Thompson, C. B., and Tsujimoto, Y. (2004) Role of Bcl-2 family proteins in a non-apoptotic programmed cell death dependent on autophagy genes. *Nat. Cell Biol.* **6,** 1221–1228

51. Pyo, J. O., Jang, M. H., Kwon, Y. K., Lee, H. J., Jun, J. I., Woo, H. N., Cho, D. H., Choi, B., Lee, H., Kim, J. H., Mizushima, N., Oshumi, Y., and Jung, Y. K. (2005) Essential roles of Atg5 and FADD in autophagic cell death: dissection of autophagic cell death into vacuole formation and cell death. *J. Biol. Chem.* **280,** 20722–20729

52. Yousefi, S., Perozzo, R., Schmid, I., Ziemiecki, A., Schaffner, T., Scapozza, L., Brunner, T., and Simon, H. U. (2006) Calpain-mediated cleavage of Atg5 switches autophagy to apoptosis. *Nat. Cell Biol.* **8,** 1124–1132